

Analysis of long crack lines in paper webs

L.I. Salminen^{1,a}, M.J. Alava¹, and K.J. Niskanen²

¹ Helsinki University of Technology, Laboratory of Physics, PO Box 1100, 02015 HUT, Finland

² KCL Science and Consulting, PO Box 70, 02151 Espoo, Finland

Received 9 December 2002

Published online 11 April 2003 – © EDP Sciences, Società Italiana di Fisica, Springer-Verlag 2003

Abstract. We analyze 6500 mm long fracture lines of paper as an example of crack propagation involving disorder. The cracks are asymptotically self-affine, with a roughness exponent close to 0.6. Systematic deviations from the power-law-scaling exist below a lengthscale related to the microscopic heterogeneities and possibly to a cross-over from 3d to 2d crack propagation. Several analysis methods are discussed, including first return analysis and the detection of correlated trends.

PACS. 62.20.Mk Fatigue, brittleness, fracture, and cracks – 81.40.Np Fatigue, corrosion fatigue, embrittlement, cracking, fracture and failure – 05.40.-a Fluctuation phenomena, random processes, noise, and Brownian motion – 62.20.Fe Deformation and plasticity (including yield, ductility, and superplasticity)

1 Introduction

In the end of any tensile test a crack propagates through the sample and thus a fracture line is created. The rupture process is decisive to properties of the crack line [1, 2], particularly in the presence of disorder. Local stiffness variations, narrowing of stress field with increasing crack velocity, and coalescing of microcracks can all interact, in a mostly unknown manner.

Paper is an example of an industrial product with many kinds of structural non-uniformity [3]. Starting from the fiber network structure, the positions and orientations of fibers are random. The fibers are 1–3 mm long. There are 10–20 layers of fibers in an ordinary paper of typical thickness 100 μm . Thus the sheet structure becomes quite uniform over areas of the order of 1 mm². At smaller scales, paper is a three-dimensional porous material whose structure is controlled by the width (2–10 μm) and thickness (10–50 μm) of fibers [4]. At these small length scales the rupture of paper involves interfiber bond rupture and fiber pull-out competing with fiber rupture [5]. The effect of fiber properties and sheet structure on paper strength can be described for engineering purposes using linear elastic fracture mechanics modified to account for the plastic yielding that arises from the gradual debonding of fibers [6]. At fiber lengths and above, 1–10 mm, the mass distribution of paper is non-uniform because of flocculation. This non-uniformity is easily seen in the “grainy” or “cloudy” pattern when viewing *e.g.* a copy paper against light. The variation is usually rather weak, below 10 % of the mean mass. Due to the manufacturing process,

the non-uniform mass distribution is connected with non-uniform residual stresses, and the combination of the two controls the crack line pattern that is created when one tears a paper sheet apart. In general the behavior of paper is brittle and nearly linearly elastic for strains upto 1%. The elastic properties and breaking thresholds exhibit variations at all length scales from 1 cm up to the width of the full paper machine web, 10 m. As a material it presents a good example of the influence of disorder, in a quasi 2d geometry, and for instance the possible relation of crack surface roughness and fracture toughness would be of practical and theoretical interest [7].

Especially interesting from the statistical physics viewpoint are crack line properties that obey power-law behavior, a concept launched by Mandelbrot and co-authors in the 80’s [1]. The most classical feature is the fact that mechanisms producing power-laws do not have any characteristic scale. Self-affinity or fractal dimension is an example of power-law phenomenon observed experimentally in several fronts. Because of complicated microstructure, in the case of paper the actual self-affinity has not been proved conclusively [8,9]. Computer simulation has been used for simple models to study 2d fractography. This is due to the ease of such models, both conceptually and numerically given the existence of suitable methods for solving the systems of equations. Examples are random-fuse, random-beam, and random-fiber models [10]. The outcome of Monte-Carlo computer simulations is usually a crack line with a variable amount of branching, and one should keep in mind that the stress-strain behavior used is able to mimic only materials with extreme brittleness (like glass) [11].

^a e-mail: lsa@fyslab.hut.fi

Simulations of 2D statistical models give rise to power-laws that result in roughness exponents χ in the range 0.7 to 0.85 for slow, quasi-static fracture [10]. The exponent χ can be measured by many different statistical aspects of crack lines, as discussed below. For minimum (fracture) energy surfaces the roughness exponent is $2/3$, exactly, while numerical simulations of random fuse networks result in values close to that (about 0.7) [10]. These are both in contrast to beam networks where typically somewhat larger exponents are obtained. In analogy, it is of interest to explore the range of true power-law scaling in paper, and its relation to the formation or evenness of paper.

All possible choices of χ (expected on the basis of different universality classes) of roughness exponent χ would usually lie between 0.5 and 0.9. Only a few 2d experimental values have been established [12], including a set of exponent values by Kertesz *et al.* [9]. They observed for 300 mm wide tensile test sheets of paper a Hurst exponent between 0.63 and 0.72. This range of values for roughness exponent for paper stressed in machine direction is as such large. They also suggested that due to entanglement the fibers are forced to break even though their strength is much higher than the strength of bonds. Kertesz *et al.* also proposed that bond breakages are the origin of plasticity. This is in contradiction with the common belief, that very few breakages take place before the maximum stress despite sometimes high, order of 0.3 per cent, amount of plastic strain.

Bouchaud suggested in her review that 3d materials give always an asymptotic global roughness exponent 0.8 [2], and that for slow fracture, at very small length scales the exponent value can be smaller, of the order of 0.5. The time-dependent behavior would be a consequence of crack front pinning/depinning. In this situation the external force is close to a critical force so that the crack is just able to free itself from microstructural obstacles. The higher the crack velocity the smaller is the length-scale that separates the depinning transition regime and universal roughening regime. It might also be so that the correlation length, the limit of power law behavior matches with the largest heterogeneity of the material. Notice that such ideas are relevant for slow fracture, but for time-dependent roughening processes the possible theoretical outcomes are mostly unknown.

The effect of the velocity of the crack tip [13], and the length of possible pinning periods have been widely discussed in literature in the context of fast fracture [14,15]. Rapid crack advancement is usually proposed to produce a straight crack path, but in particular one should note that the experiments have been performed on brittle materials (*e.g.* PMMA) with weak disorder. In addition to conventional rupture line analysis some indirect measurements are possible. The propagation of crack can be monitored by acoustic emission, and in some special cases the origin of the sound, the position of cracktip, can be traced [15].

During statistical analysis of rupture lines the question of tilt removal arises and should be handled carefully [16]. This means that the fracture surface can have macroscopic trends that may or may not be connected to the mecha-

nism that leads to roughening. Subtracting the difference of the end-and-start points (or removing a linear trend) is not necessarily sufficient or justified, and can overrule underlying details. Fortunately for small sample sizes, typical in microscopic studies, the existence of such trends is unimportant.

Due to the multitude of open questions it is worth considering the simplest model for the formation of fracture lines: a plain random walk (RW) of the crack tip in the direction transverse to its propagation. This limit can be taken if the inhomogeneity of the stress-field of the whole crack can be neglected. In the opposite limit, the process could resemble in the quasi-static limit a Laplacian random walk [17]. A RW represents a Markov process that has equal and independent jump probabilities to all principal directions, in particular here along the crack axis and perpendicular to that. If the roughening of a 2D fracture line would be described by random walk one would get a $\chi = 1/2$, possibly masked by the fact that the events involve certain length-scales, *e.g.* the fracture leaps mentioned above. The masking would reflect the microscopic character of the medium, here paper, and is not a priori reproduced by a RW. If one considers the crack surface as a trail of the crack tip, one can compare the increments in the discrete height profile h_i . Deviations from a random walk imply that some combination of the following effects is at play: 1) the increments have a very wide distribution (as in Lévy-walks), 2) the increment amplitudes are correlated, and 3) the signs of the increments have correlations (*e.g.* as in fractional Brownian motion). In cases 2) and 3) the correlations have to be decay slowly enough to change the scaling from a simple RW.

In this paper we discuss the roughness of cracks using three paper samples obtained from two industrial paper-machines. In the next section, we describe the situation from which the samples were obtained, and the procedure to obtain the crack line to be analyzed. Section 3 discusses the results concerning the roughness properties. Our main results are i) the existence of short-range (SR) effects on a scale that relates to a cross-over to 2d propagation, and ii) asymptotic self-affine scaling. The final section finishes the paper with conclusions.

2 Samples

The whole 6.5 m wide paper web was broken by hitting the edge of the web with a rod just before the reeling. The “pulling” end of the paper web could be collected afterwards from the reel surface. This gave us practically wrinkle-free crack-line specimens that span across the whole web. The macroscopic stress state during the crack propagation is complicated because the web movement (at ca. 20 m/s) gives rise to out-of-plane disturbances (“flutter”). The random dynamic disturbances may have influenced the crack lines and contributed to the differences between the samples at large length scales. The whole rupture process takes less than 1 s, giving a lower bound of 10 m/s for the crack velocity. This is far below the Rayleigh-velocity, but one should note that the breaks

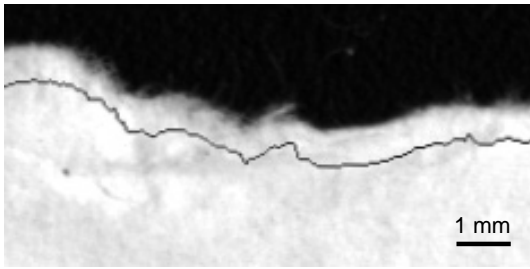


Fig. 1. Example of crack line detection (crackline 1). The image width 10 mm. The detected edge is marked by a dark line which is shifted for clarity by 0.6 mm downwards.

are nonetheless unstable because the whole web ruptures always when one applies even a small cut at the edge.

The two paper machines use the same fibrous raw material. There are only small (10%) differences in the mean mechanical properties of the papers that are produced on the two paper machines and the ranking of the samples depends on the property concerned. It is therefore probable that the eventual differences in the crack line properties arise either from the machine-induced inhomogeneities above 1 mm, or from the uncontrolled tension variations and out-of-plane deviations (“fluttering”) of the web.

We study various statistics of the height profiles of the rupture lines. Each crack line is scanned with a flatbed scanner of 600 dpi resolution with 256 gray levels and a black background. The complete crack line is composed of about 30 individual images. Images overlap slightly and are merged so that angle between images is taken into account. The difficulties in joining images may produce some distortion, but such errors are considered to be negligible. The crack line is detected by thresholding gray level gradient. First we calculate the histogram of gray values. Since the paper is white and the images are taken with a black background, we search for the deepest valley between the histogram peaks of the paper and the background. If several crack branches are present we choose the outmost one. The so-called solid-on-solid approximation is also applied. By this practice we are able to extract the single-valued crack line with minimal assumptions. Figure 1 shows a sample of one of the cracklines, on a scale that allows to observe the variation of the grey levels across the crack. Superimposed on the plot there is the actual crackline as constructed by the thresholding method. Note the absence of any single-fiber related effects in the final profile, in particular overhangs due to fibers sticking out of the crack.

The crack lines consist of about 160 000 points, each point corresponding to 0.042 mm. With this resolution we cannot distinguish individual fiber ends sticking out of the crack line and therefore cannot see the small “overhangs” that the randomly oriented fiber ends create [18]. Crack line branching is only moderate, contrary to some computer simulations. We do not quantify the phenomenon, but note that of the order of 1 short (less than 10 mm) branches are found per 1 meter of the backbone of the rupture line. The crack lines show variation in different length

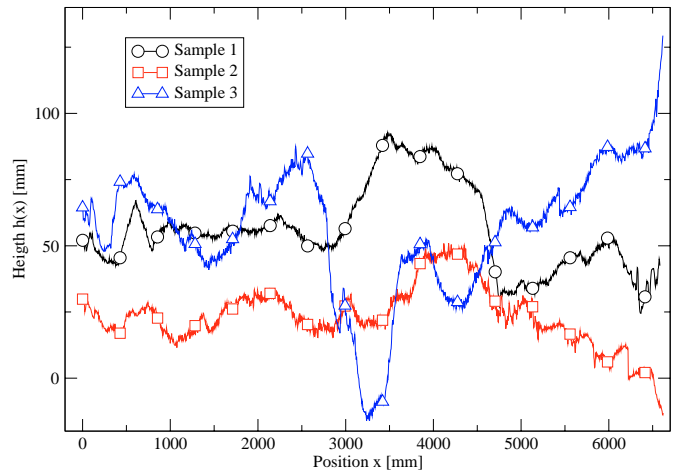


Fig. 2. Crack lines for all the samples.

scales (Fig. 2). Any kind of analysis we applied was unable to distinguish the crack propagation direction.

The extracted crack line is analysed as a 1-d series. The global mean height is subtracted before any amplitude sensitive measurements. We consider the crack lines with several different methods. First we calculated the roughness and roughness exponent then we introduce several other ideas for analysis. Note that no time information (temporal) is available, thus in this study we only discuss the a posteriori rupture properties.

3 Fracture surface properties

The roughness *i.e.* standard deviation of height *vs.* measurement window size l is a simple way to measure the shape of crack line. The power-law nature of roughness makes it possible to determinate the roughness exponent χ . Unfortunately that method is vulnerable to anomalies in data [16]. Distortions like global tilt, or periodic oscillations can affect the slope determination. Other methods of roughness exponent estimation like z_{max} , return probability, Fourier Power Spectrum, and wavelet analysis are also available [2]. In practice the roughness exponent χ is handy, but quite an inaccurate measure of fractal properties.

The max difference method is grounded on the fact that the difference between the lowest and highest value within certain window r scales as a function of the window size with the relationship $z_{max} \sim r^\chi$ [2]. This method is painless and in general reliable, but can be distorted by tilts on very large scales, above any correlation length. Figure 3b shows roughness with maximum difference *i.e.* z_{max} method. The bumps (in Fig. 3a) or the change of slope (Fig. 3b) on the scale of 1 to 5 mm could arise from either the non-uniformity of mass distribution or from a cross-over between three-dimensional fracture surfaces at small scales and two-dimensional crack lines at large scales.

The Fourier power spectrum measures the amplitude of oscillations, thus it is evident that the roughness exponent can be easily extracted. Contrary to Fourier analysis, the wavelet analysis can obtain both spatial and spectral

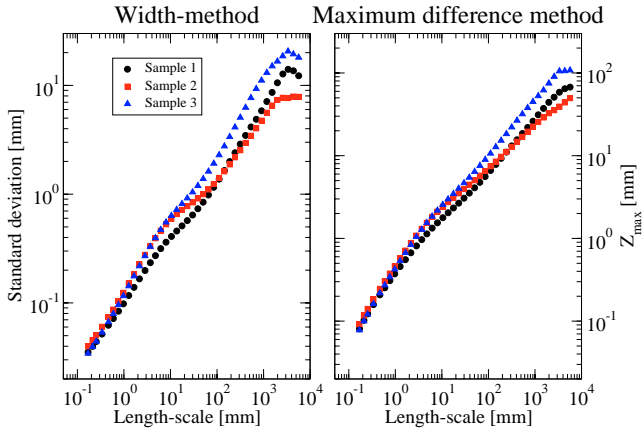


Fig. 3. Roughening of crack lines by standard deviation-method and Z_{max} -method.

Table 1. Roughness exponent χ with different methods.

Method	Sample 1	Sample 2	Sample 3
Standard dev.	0.63 ± 0.03	0.53 ± 0.02	0.665 ± 0.009
Wavelet	0.62 ± 0.02	0.539 ± 0.005	0.619 ± 0.008
Power Spect.	0.61 ± 0.10	0.51 ± 0.06	0.64 ± 0.09
Z_{max}	0.634 ± 0.007	0.53 ± 0.02	0.664 ± 0.004
DFA	0.698 ± 0.005	0.61 ± 0.06	0.666 ± 0.004
Average	0.64 ± 0.03	0.54 ± 0.04	0.65 ± 0.02

resolution simultaneously. The wavelet analysis is however less simple to interpret [19]. The tilts and average height can give some distortion to both Fourier and wavelet analysis, since the resulting coefficients represent literally the original data sequence. Finally we apply the detrended fluctuation analysis (DFA) [20] to the data. This is based on dividing the available data series into windows, and subtracting in each of these the trend, locally. The results of the method turn out to be analogous to the other techniques employed.

For the roughness exponent we obtain the values 0.64 ± 0.03 , 0.54 ± 0.04 and 0.65 ± 0.02 for samples 1, 2, and 3, fitted over the most of the range of available data. The error estimates are based on the variation with the fitting window choice (Tab. 1). The more local values of χ are typically equal to the “global ones” (maximal window) and the variation is order of ± 0.05 if constrained upto a 700 mm wide window. For very large length-scales χ varies by about 0.05 across to all the scaling.

Our conclusion about roughness analysis is an observed exponent value $\chi = 0.60 \pm 0.10$. This value is not comparable with values expected based on the literature, since it is both *above* the RW value and slightly *below* the slow fracture simulation model results. Therefore, the question arises: since the front is a consequence of crack tip propagation, how are its fluctuations correlated and are there any other measures than the roughness exponent, that could yield information on the dynamics?

For small roughness values w (*e.g.* as measured by the standard deviation methods) one has to consider the influence of any structural details on the same scale. To this

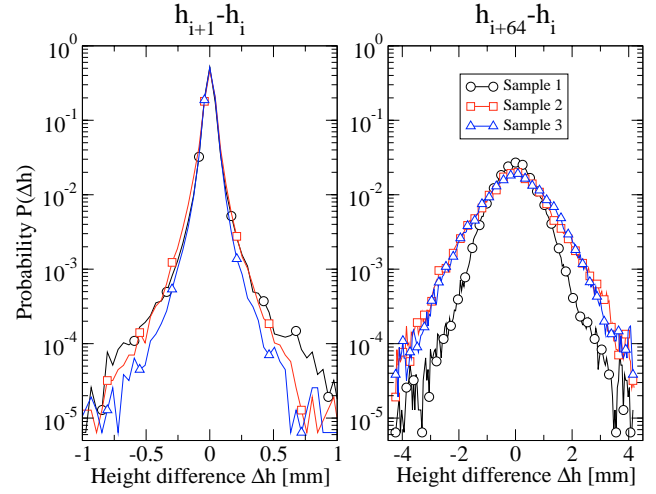


Fig. 4. Distribution $P(\Delta h)$ of height differences $\Delta h = h_i - h_{i+1}$ (left figure) and $\Delta h = h_i - h_{i+64}$ (right figure).

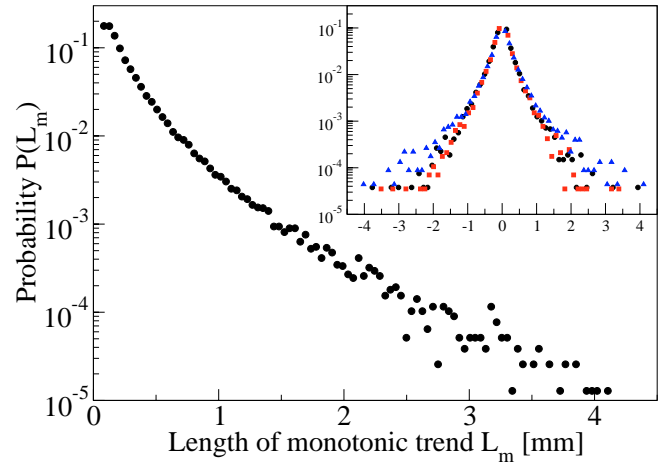


Fig. 5. Length distribution of monotonic trends for the combination of samples 1, 2, and 3. Subfigure shows directed length distributions for each sample.

end, we compute the front height differences $\Delta h(L) = \langle h_i - h_{i+L} \rangle$ for different window lengths L to describe the short scale behavior of fracture. Very large changes in height are rare and the distribution becomes finally close to a normal distribution (Fig. 4 for $L = 1$ (0.042 mm) and $L = 64$ (2.7 mm) pixels) with increasing L . The histograms are close to symmetric, and the skewness is small. Such steps as measured by Δh may or may not be *correlated* over some lengthscale ξ as outlined before.

Both any naive picture of an advancing crack tip and the random walk analogies make it natural to measure the “persistence” or the local trends in the crack line. Thus we next investigate the statistics of monotonic regions in the crack lines. Such a region is a continuous sequence of either positive or negative height changes, say $h_i \geq h_{i+1}$. For a RW such a distribution is exponential (straight line in Fig. 5). Evidently the distribution in our samples is not

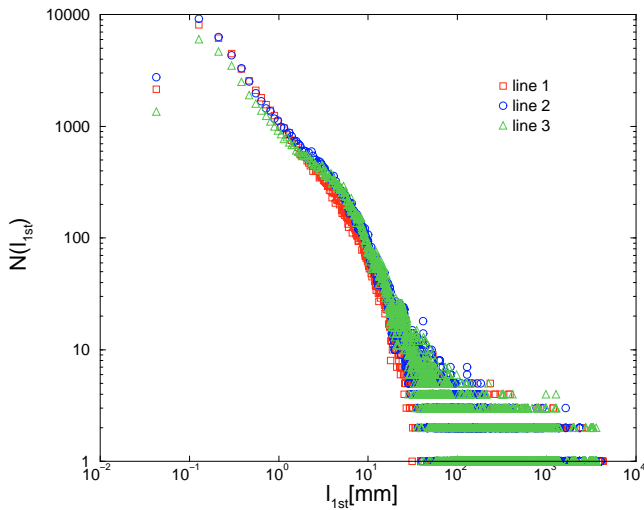


Fig. 6. First-return histograms for the samples 1, 2, and 3.

exponential. This implies either an increasing tendency to continue to the same direction or *e.g.* a cross-over from 3d effects to purely 2d propagation. This analysis is very sensitive to global height trends on the scale that the statistics would indicate. An analysis of the auto-correlation function of the increments $\Delta h(1)$ indicates that the step-step correlations vanish over a lengthscale of about 1 mm, that is, close to the fiber length. The first-return properties $P_{1st}(r)$ of the surfaces are measured for all x_0 , by the distance at which the interface returns for the first time to the position at x_0 . That is, if $r(x) = r_0$ it implies that *e.g.* $h(y) > h(x_0)$ for $x_0 < y < x + r_0$, and $h(x + r_0) \leq h(x)$. $P_{1st}(r)$ are shown in Figure 6. At short scales, they are in qualitative agreement with *e.g.* the z_{max} method. The data implies an effective roughness exponent closer to unity, than the overall χ , slightly above 0.85 perhaps. This could be taken to imply that the cracks are actually three-dimensional on short scales due to the similarity with the “universal” 3d roughness exponent [2]. On scales up from several millimetres the first return properties seem to reflect more the large-scale trends than the self-affine properties. For a self-affine signal the expectation is $P_{1st}(r) \sim r^{2-\chi}$ [21]. The values of r are as a matter of fact sometimes highly correlated, due to the large-scale variations of the fracture lines (see Fig. 2) that induce correlations in x among the large $r(x)$ -values.

A more robust similar statistics for the trends in the fluctuations is to fit straight lines with varying window size and calculate the standard deviation of the slopes (Fig. 8). The method results in a series of slopes k_i , such that since the window is moved by one pixel at a time the values of k_i are evidently correlated. By comparing two values k_j, k_m such that $|m - j|$ equals the window size one can analyze coarse-grained trends in the crack line on a scale defined by the window. The difference $k_j - k_m$ tells about how the slope changes on such a scale, and can be compared *e.g.* to randomized differences obtained from $P(k, l)$. Figure 7 shows that sample 2 has strong fluctuations up to a lengthscale of about 5 mm, after which

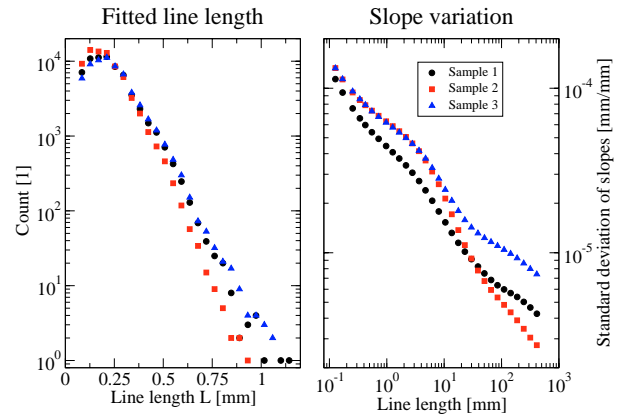


Fig. 7. On the left distribution of the length of straight lines. On the right the standard deviation of least square fit slope with varying fit length.

the variation drops rapidly. In samples 1 and 3 we notice a lower level of fluctuations. Such scales might be related to the so-called floc size in paper [22] or to differences in the state of the web during the fracture. Note that the trends are similar in samples 1 and 3, which also exhibit similar roughness scaling by all the methods tested.

Another idea of analysis is a method that fits series of lines with varying lengths by the least squares method, so that the length of the line is increased by one as long as the largest deviation between the line and the data is less than 0.5 pixel. The idea is based on the fact that scanned crack lines are digitized to integer height values. We start at h_0 with line length $l = 2$. After that we set the starting point to the end of the previous line and start fitting a new line. A series of straight lines is fitted to data so that by rounding the original height profile is reconstructed completely. The distribution of line lengths is similar in samples 1 and 3 and clearly different in sample 2 (Fig. 7). The decay of the variation with line length is in reasonable agreement with the idea, that the slopes on scale l are related to the ratio l^χ/l , in all the three cases separately, even, as one would expect given that the average slope of such lines should be proportional to the roughness in the given window.

4 Summary

To conclude, we have investigated the roughness properties of three very large samples of 2D crack surfaces. The material, industrial paper, contains disorder which interacts with an advancing crack. It is a matter of taste whether one considers the data to imply that all the samples have the same exponent, or that in one the exponent is slightly lower and close to the RW one. We obtain for all the samples that the roughness is of power-law type, with an exponent that is larger than a pure RW value, and slightly below of what one might expect for slow static fracture in 2D. Recall that for minimum energy surfaces $\chi_{2d} = 2/3$, while for scalar fracture models the effective exponent is of the order of 0.7 [10]. In this respect, it may

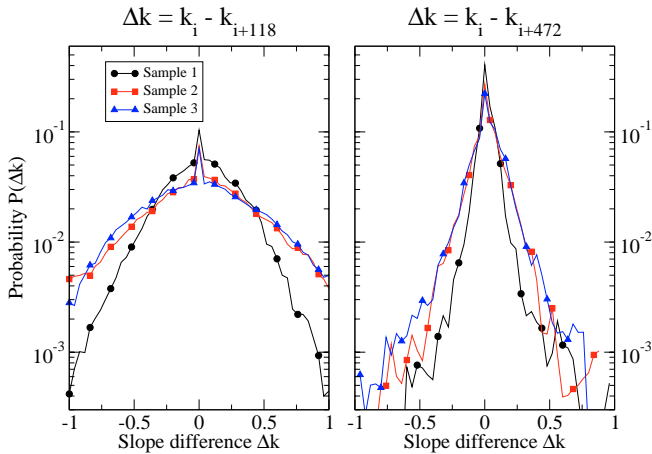


Fig. 8. Distribution of subsequent slope differences for $L = 5$ mm and $L = 20$ mm.

again be of importance that one of the samples exhibits a smaller value of χ , in general. These models would assume slow, quasi-static growth dynamics which evidently is not valid, at least strictly speaking.

The actual differences in the measured quantities and among the samples can be traced to two separate origins. The effect of the different length scales (3d fracture on short distances, local structure fluctuations over a few mm at most) is reflected in all the three samples. In particular, the short-scale scaling of the roughness seems sometimes directly to imply a χ_{SR} which is close to the 3D static fracture one (0.8) [2]. It seems likely that the sample-to-sample variations reflect not any microscopic material differences, but the varying stress states during the three fracture processes. These may originate eg. from the air flows (“fluttering”) peculiar to each case, that produce out-of-plane fluctuations.

The scale invariance is in line with the qualitative observations about trends in the lines. The microstructural aspects can be noticed in the roughness statistics as well: the crack lines have large jumps on the discretization scale, and the asymptotic scaling is only obtained beyond any fluctuation scale that would overlap with the jump sizes. This is similar to what has been observed for fracture surfaces in polymers [23]. Our results have further theoretical implications: an unstable crack interacting with disorder creates rough surfaces, in the presence of no extensive branching. The first-return properties and the statistics of trends present interesting issues for further study.

MA and LS would like to thank the Academy of Finland, Center of Excellence program for financial support.

References

1. B.B. Mandelbrot, D.E. Passoja, A.J. Paullay, *Nature (London)* **308**, 721 (1984)
2. E. Bouchaud, *J. Phys. Cond. Mat.* **9**, 4319 (1997)
3. *Paper Physics*, edited by K.J. Niskanen (Fapet, Helsinki, 1998)
4. K. Niskanen, H. Rajatorja, *J. Pulp Paper Sci.* **28**, 228 (2002)
5. H. Kettunen, Y. Yu, K. Niskanen, *J. Pulp Paper Sci.* **26**, 260 (2000)
6. K. Niskanen, H. Kettunen, Y. Yu, *The science of paper-making*, Vol. 2, (The Pulp and Paper Fundamental Research Society, Bury, UK, 2001), pp. 1467–1482
7. S. Morel, J. Schmittbuhl, E. Bouchaud, G. Valentin, *Phys. Rev. Lett.* **85**, 1678 (2000)
8. J. Rosti *et al.*, *Eur. Phys. J. B* **19**, 259 (2001)
9. J. Kertész, V.K. Horvath, F. Weber, *Fractals* **1**, 67 (1993)
10. V.I. Räsänen *et al.*, *Phys. Rev. Lett.* **80**, 329 (1998); E.T. Seppälä, V.I. Räsänen, M.J. Alava, *Phys. Rev. E* **61**, 6312 (2000); B. Skjetne, T. Helle, A. Hansen, *Phys. Rev. Lett.* **87**, 125503 (2001); A. Hansen, J. Schmittbuhl, *Phys. Rev. Lett.* **90**, 045504 (2003)
11. See: L.I. Salminen, A.I. Tolvanen, M.J. Alava, *Phys. Rev. Lett.* **89**, 185503 (2002) for some comments on how paper fracture compares with such models, in particular if monitored with acoustic emission
12. T. Engoy, K.J. Maloy, A. Hansen, *Phys. Rev. Lett.* **73**, 834 (1994)
13. F. Plouraboué *et al.*, *Phys. Rev. E* **53**, 277 (1996) supports actually the idea that constant-velocity crack propagation leads to identical roughness scaling, at least for small velocities
14. J. Fineberg, M. Marder, *Phys. Rep.* **313**, 1 (1998)
15. J.F. Boudet, S. Ciliberto, *Phys. Rev. Lett.* **80**, 341 (1998)
16. J. Schmittbuhl, J. Vilotte, S. Roux, *Phys. Rev. E* **51**, 131 (1995)
17. J.W. Lykelma, C. Everetsz, L. Pietronero, *Europhys. Lett.* **2**, 77 (1986)
18. H. Kettunen, K. Niskanen, *J. Pulp Paper Sci.* **26**, 35, (2000)
19. I. Simonsen, A. Hansen, O.M. Nes, *Phys. Rev. E* **58**, 2779 (1998)
20. C.-K. Peng, S.V. Buldyrev, S. Havlin, M. Simons, H.E. Stanley, A.L. Goldberger, *Phys. Rev. E* **49**, 1685 (1994); K. Hu, P. Ch Ivanoc, Z. Chen, P. Carpena, H.E. Stanley, *Phys. Rev. E* **64**, 011114 (2001)
21. S.N. Majumdar, A.J. Bray, *Phys. Rev. Lett.* **86**, 3700 (2001)
22. N. Provatas, M.J. Alava, T. Ala-Nissilä, *Phys. Rev. E* **54**, R36 (1996)
23. F. Lapique, P. Meaking, J. Feder, T. Jossang, *J. Appl. Polymer Sci.* **86**, 973 (2002)